

Semantic Segmentation on VSPW Dataset through Masked Video Consistency

Chen Liang^{1,2*} Qiang Guo^{1*} Chongkai Yu¹ Chengjing Wu¹ Ting Liu¹ Luoqi Liu¹
¹MT Lab, Meitu Inc.

²Chinese Academy of Sciences, Institute of Automation

{lc25, gq5, yck, ethan, lt, llq5}@meitu.com

Abstract

Pixel-level Video Understanding requires effectively integrating three-dimensional data in both spatial and temporal dimensions to learn accurate and stable semantic information from continuous frames. However, existing advanced models on the VSPW dataset have not fully modeled spatiotemporal relationships. In this paper, we present our solution for the PVUW competition, where we introduce masked video consistency (MVC) based on existing models. MVC enforces the consistency between predictions of masked frames where random patches are withheld. The model needs to learn the segmentation results of the masked parts through the context of images and the relationship between preceding and succeeding frames of the video. Additionally, we employed test-time augmentation, model aggregation and a multimodal model-based post-processing method. Our approach achieves 67.27% mIoU performance on the VSPW dataset, ranking 2nd place in the PVUW2024 challenge VSS track.

1. Introduction

The PVUW2024 VSS Track focuses on the Pixel-level Video Understanding in the Wild (Miao et al., 2021, 2022), which is a critical task in advancing computer vision. Unlike traditional image segmentation, this challenge addresses the need for video segmentation, recognizing that real-world applications are video-based rather than static. The goal is to assign predefined semantic labels to every pixel in all frames of a given video, leveraging temporal information to improve predictive accuracy. This task is more challenging than image-based segmentation since it requires the integration of spatial and temporal data to produce accurate and stable semantic information across continuous frames. The final evaluation is conducted on the VSPW (Miao et al., 2021) dataset, with using mean Intersection over Union (mIoU) and Video Consistency (VC) as

evaluation metrics.

However, existing methods (Zhang et al., 2023a,b) face several challenges: they struggle with finely segmenting object edges, often misclassifying regions of the same object with nearly unchanged visual features in the original image as different categories. Additionally, their capability for temporal modeling remains underdeveloped, resulting in the model’s inability to maintain stable segmentation of the same semantic category across adjacent frames. To address these issues, we introduce Masked Video Consistency (MVC). MVC optimizes existing models by enforcing consistency constraints in both temporal and spatial dimensions. It encourages the model to maintain consistent predictions for masked frames, where random patches are hidden, by leveraging the contextual information from surrounding frames and the spatial structure of the video. This dual-focus on spatial and temporal consistency aims to overcome the limitations of current models and achieve more accurate and stable video semantic segmentation.

To alleviate the burden during the model training process, we employed a Test-Time Augmentation (TTA) strategy that integrates segmentation results from various input modifications using a single model, rather than assembling multiple models. Specifically, we applied different input scales and image flips. This approach allows us to leverage the strengths of multiple augmented views of the input data, enhancing the robustness and accuracy of the segmentation results without the additional computational overhead of training and maintaining multiple models. By using TTA, we ensure that our model can generalize better to diverse input conditions, leading to more reliable performance in practical applications.

In the post-processing stage, we utilized the large multimodal model (Liu et al., 2023, 2024; Achiam et al., 2023) to correct some of the video segmentation results. During our observation of the final segmentation outcomes, we found that the model struggled to maintain consistency in segmenting challenging stuff classes across the entire video sequence. Additionally, it sometimes misclassified a single class into multiple similar class regions within a single

*Equal contribution.

frame. We attributed this issue to the model’s lack of sufficient training data. To address this, we employed a large multimodal model to refine these results, ultimately ensuring consistent segmentation throughout the entire video.

By combining the above strategies, we achieved a 67.27% mIoU on the final test set. Additionally, VC₈ and VC₁₆ scores were 94.99% and 93.12%, respectively, demonstrating the consistency and stability of our segmentation results.

2. The proposed method

2.1. Baseline Model

DVIS++ (Zhang et al., 2023b) is a general-purpose video segmentation model that has achieved state-of-the-art performance across various benchmarks, including video instance segmentation, video semantic segmentation, and video panoptic segmentation. Therefore, we chose DVIS++ as the baseline model for our experiments and explored its capabilities further. Unlike previous models with end-to-end training, DVIS++ decouples video segmentation into three cascaded sub-tasks: segmentation, tracking, and refinement. This task-decoupling design allows us to separately explore the temporal and spatial consistency brought by Masked Video Consistency (MVC).

2.2. Masked Video Consistency

To accurately identify an object or region, a model typically needs to utilize clues from different parts of an image. These clues can come from the local information of the same image block corresponding to the units in the feature map, or from the surrounding image blocks, corresponding to the contextual information of the image (Hoyer et al., 2019). Additionally, for temporal modeling tasks such as video segmentation, the image information from other video frames also constitutes a crucial temporal context.

Many network architectures (He et al., 2016; Dosovitskiy et al., 2020) have the capability to integrate local and contextual information into their features. However, they struggle to effectively enforce the learning of useful context clues. Our experiments have shown that while DVIS++ models inter-frame relationships within a unified video through the Referring Tracker and Temporal Refiner, it still exhibits instability in the final segmentation results. To inject more contextual clues into the model, we propose the plug-and-play Masked Video Consistency (MVC) approach.

Specifically, for each image, a patch Mask \mathcal{M} is obtained by

$$\mathcal{M}_{ij} = [v > r] \quad \text{with} \quad v \sim \mathcal{U}(0, 1) \quad (1)$$

where $[\cdot]$ denotes the Iverson bracket, b is the patch size, r is the mask ratio, i and j represent the positions of image blocks. The masked image is obtained by element-wise multiplication of mask and image

$$x^M = \mathcal{M} \odot x^T \quad (2)$$

The final prediction \hat{y}^M is inferred from the images that were removed from a portion of the mask

$$\hat{y}^M = f_{\theta}(x^M) \quad (3)$$

The final loss function obtained for model training is as follows

$$\min_{\theta} \frac{1}{N} \sum_{k=1}^N (\mathcal{L}_k + \lambda \mathcal{L}_k^M) \quad (4)$$

The loss \mathcal{L} is defined according to the baseline model.

2.3. Model aggregation

Furthermore, we combined the segmentation results of two models: one trained with the Masked Video Consistency (MVC) strategy and one trained without it. This dual-model approach aims to mitigate the potential instability introduced by MVC when there are significant differences between consecutive video frames (e.g., non-continuous frames). We leverage optical flow to measure the temporal consistency of the segmentation maps.

Given two consecutive frames from a video, x_t and x_{t+1} , we compute the optical flow using Farneback method (Farneback, 2003).

$$\mathbf{F}_{t \rightarrow t+1} = \text{OF}(x_t, x_{t+1}) \quad (5)$$

where $\mathbf{F}_{t \rightarrow t+1}$ represents the optical flow from x_t to x_{t+1} , OF is the Farneback method (Farneback, 2003).

With obtaining optical flow $\mathbf{F}_{t \rightarrow t+1}$, we then warp the segmentation result y_t to generate the prediction of frame x_{t+1}

$$\tilde{y}_{t+1} = \text{Warp}(y_t, \mathbf{F}_{t \rightarrow t+1}) \quad (6)$$

To evaluate the quality of the segmentation, we compare the warped segmentation map \tilde{y}_{t+1} with y_{t+1} using the Structural Similarity Index (SSIM)

$$\text{SSIM}(\tilde{y}_{t+1}, y_{t+1}) = \frac{(2\mu_{\tilde{y}_{t+1}}\mu_{y_{t+1}} + C_1)(2\sigma_{\tilde{y}_{t+1}y_{t+1}} + C_2)}{(\mu_{\tilde{y}_{t+1}}^2 + \mu_{y_{t+1}}^2 + C_1)(\sigma_{\tilde{y}_{t+1}}^2 + \sigma_{y_{t+1}}^2 + C_2)} \quad (7)$$

where μ and σ represent the mean and variance of the respective segmentation maps, and C_1 and C_2 are constants to stabilize the division.

We repeat the above process for both sets of segmentation results. The segmentation result with the higher SSIM score is considered to be temporally more consistent and, thus, of higher quality. We select each video based on this strategy for the segmentation results of the two models, and ultimately obtain the integration results of the two models.

2.4. Test-time augmentation

We utilized test-time augmentation to integrate segmentation results from the same model with different inputs, including stochastic flipping and multi-scale data enhancement. The scales used in multi-scale inference include 0.9, 1.0, 1.1, 1.2, and each scale involves horizontal flipping.

After obtaining multiple model predictions, we integrated the results using a voting approach. For each pixel in each image, we perform voting across all prediction results. In the event of a tie, we prioritize the result corresponding to the higher resolution input, as high-resolution inputs potentially contain more image details, which facilitates model analysis and inference.

For each pixel j , the final prediction result V_j can be expressed as:

$$V_j = \begin{cases} \text{mode}(\{y_{i,j} \mid i = 1, 2, \dots, N\}) & \text{if no tie} \\ y_{i^*,j} & \text{if tie} \end{cases} \quad (8)$$

where the mode function calculates the most frequent class in the set, N represents the total number of different augmentations, and i^* is the index corresponding to the high-resolution input in the augmentation set. By TTA, the reliability of the final results is further enhanced.

2.5. Post-processing

Although the aforementioned method enhances the model’s ability to utilize existing information, such as learning the patterns corresponding to each category from the training set images and learning the inter-frame correspondence in video sequences, it is still limited by the finite scenes in the VSPW training set. As a result, the model struggles to generalize to unseen scenes. In our experiments, we observed that while the model produced relatively complete segmentation masks for some challenging scenes, it tended to make classification errors in the masks for categories that could be ambiguous. To address these issues, we attempted to use a large multimodal model (Liu et al., 2023, 2024; Achiam et al., 2023) to post-process the segmentation results, leveraging its extensive and rich training samples.

3. Experiments

3.1. Datasets and evaluation metrics

VSPW (Miao et al., 2021) is a dataset with the target of advancing the scene parsing task for images to videos.

VSPW contains 3,536 videos, including 251,633 frames from 124 categories. Each video contains a well-trimmed long-temporal shot, lasting around 5 seconds on average.

We use Mean IoU (mIoU) to evaluate the segmentation performance. To evaluate the stability of predictions, we also provide experimental results of Video Consistency (VC). The evaluation metrics are consistent with the leaderboard metric of the competition.

3.2. Implementation details

We use DVIS++ (Zhang et al., 2023b) as our baseline model, which employs Mask2Former (Cheng et al., 2022) as the segmenter. The referring tracker utilizes six transformer denoising blocks, and the temporal refiner employs six temporal decoder blocks. We use the open-source Segmenter weights of DVIS++ for finetune and retrain the following modules with the same configuration. All experiments were conducted on eight NVIDIA V100 GPUs.

3.3. Ablation studies

Ablation study of MVC. To validate the effectiveness of the proposed Masked Video Consistency (MVC) in improving model segmentation capabilities, we conducted tests on DVIS++ using different backbones at various training stages in Tab. 1. For comparison with previous models, we trained using only the training set and calculated all evaluation metrics on the validation set. The experimental results clearly demonstrate that MVC enhances segmentation performance (mIoU) and video segmentation consistency (VC), outperforming the state-of-the-art DVIS++ (Offline) with 0.5% mIoU, 0.3% mVC, and 0.3% mVC. Additionally, we validated the effectiveness of MVC across different stages of DVIS++, achieving improvements of 0.6% mIoU, 0.7% mVC, and 0.9% mVC for the Online model as well. Notably, our approach does not introduce additional model parameters or increase training memory overhead; instead, it provides additional training cues based on the existing model.

Ablation study of extra training data. To fully utilize the existing annotated data, we expanded the original training set using the VSPW (Miao et al., 2021) open-source validation set data. Specifically, due to the difficulty in reproducing the pre-trained weights, we fine-tuned the Segmenter weights provided by the official DVIS++ repository (Zhang et al., 2023b) on the combined training and validation sets. Subsequently, we re-trained the Reference Tracker and Temporal Refiner using the fine-tuned Segmenter weights. The experimental results after augmenting the training data are shown in Tab. 2. As seen in the table, whether or not the MVC training strategy was employed, the inclusion of the validation set provided the model with

Method	Backbone	mVC ₈	mVC ₁₆	mIoU
Mask2Former (Cheng et al., 2022)	ResNet-50	87.5	82.5	38.4
Video-kMax (Shin et al., 2024)	ResNet-50	86.0	81.4	44.3
Tube-Link (Li et al., 2023)	ResNet-50	89.2	85.4	43.4
MPVSS (Weng et al., 2024)	ResNet-50	84.1	77.2	37.5
DVIS(online) (Zhang et al., 2023a)	ResNet-50	92.0	90.9	46.6
DVIS(offline) (Zhang et al., 2023a)	ResNet-50	93.2	92.3	47.2
DVIS++(online) (Zhang et al., 2023b)	ResNet-50	92.3	91.1	46.9
DVIS++(offline) (Zhang et al., 2023b)	ResNet-50	93.4	92.4	48.6
DeepLabv3+ (Chen et al., 2018)	ResNet-101	83.5	78.4	35.7
TCB (Miao et al., 2021)	ResNet-101	86.9	82.1	37.5
Video K-Net (Li et al., 2022)	ResNet-101	87.2	82.3	38.0
MRCFA (Sun et al., 2022b)	MiT-B2	90.9	87.4	49.9
CFM (Sun et al., 2022a)	MiT-B5	90.8	87.1	49.3
Video K-Net+ (Li et al., 2022)	ConvNeXt-L	90.1	87.8	57.2
Video kMax (Shin et al., 2024)	ConvNeXt-L	91.8	88.6	63.6
TubeFormer (Kim et al., 2022)	Axial-ResNet-50	92.1	88.0	63.2
MPVSS (Weng et al., 2024)	Swin-L	89.6	85.8	53.9
DVIS(online) (Zhang et al., 2023a)	Swin-L	95.0	94.3	61.3
DVIS(offline) (Zhang et al., 2023a)	Swin-L	95.1	94.4	63.3
DVIS++(online) (Zhang et al., 2023b)	ViT-L	95.0	94.2	62.8
DVIS++(offline) (Zhang et al., 2023b)	ViT-L	95.7	95.1	63.8
DVIS-M++(online)	ViT-L	95.7	95.1	63.6
DVIS-M++(offline)	ViT-L	96.0	95.4	64.3

Table 1. **Comparison of different methods on the VSPW validation set.** mVC_k means that a clip with *k* frames is used. The best results are highlighted in bold.

additional semantic knowledge, ultimately leading to better segmentation performance on the test set.

Method	Backbone	Dataset used		mIoU
		training	validation	
DVIS++(offline)	ViT-L	✓		61.6
DVIS++(offline)	ViT-L	✓	✓	62.7
DVIS-M++(offline)	ViT-L	✓		62.2
DVIS-M++(offline)	ViT-L	✓	✓	63.5

Table 2. **Ablation study of extra training data.** All results are on the test set in the final state.

Ablation study of test-time augmentation. The default test crop size for the DVIS++ model (Zhang et al., 2023b) is 720p. To evaluate whether different crop sizes and image flipping provide more effective input information for the model, we conducted separate experiments on these two TTA methods. The experimental results are shown in Tab. 3. Without flipping, using four input resolutions yielded better performance than using a single resolution. Additionally, images with reduced crop sizes also contributed to the model’s final voting results. On this basis, flipping the image can further improve the prediction results. We believe that higher resolutions help the model to segment image and video details more precisely, while lower resolutions assist the model in ignoring some class-irrelevant texture information. This also helps prevent the model from segmenting a single class area into multiple different class blocks to a certain extent.

Scale	Flip	mIoU
{1.0}		63.5
{1.0}	✓	63.6
{1.0, 1.1, 1.2}		63.9
{1.0, 1.1, 1.2}	✓	64.4
{0.9, 1.0, 1.1, 1.2}		64.1
{0.9, 1.0, 1.1, 1.2}	✓	64.4

Table 3. **Ablation study of test-time augmentation.** All results are on the test set in the final state.

Ablation study of model aggregation Based on the optical flow method, we evaluated the quality of segmentation results from different models on various videos. During the model integration phase, we selected the segmentation results with higher quality for integration. Tab. 4 shows the improvement brought by model integration. Compared to DVIS-M++, the integrated model achieved a 1.4% increase in mIoU.

DVIS++	DVIS-M++	mIoU
✓		63.6
	✓	64.4
✓	✓	65.8

Table 4. **Ablation study of model aggregation.** All results are on the test set in the final state.

Ablation study of post processing. We use a large multimodal model to correct the existing segmentation results, leveraging the advantages of the extensive training data used for the multimodal model. Tab. 5 demonstrates the comparative performance of GPT-4 (Achiam et al., 2023) and LLAVA (Liu et al., 2024) in predicting the class of objects in images. The prompt defined for this evaluation is *“Is the {stuff} in the image a {class1, class2, ...}? Please give me the only answer.”* While GPT-4 provides concise and accurate predictions, LLAVA misclassifies the water in both images as a river. GPT-4 showcases higher recognition accuracy in most of the cases. Given its superior performance in correctly classifying the objects, we adopted GPT-4 to refine segmentation results via a Q&A approach. By leveraging GPT-4’s accurate predictions, we ensure more reliable and precise segmentation corrections.

3.4. Comparison with other teams

In the final stage of the competition, our model achieved 67.3% mIoU, securing the 2nd position among all participating teams. Meanwhile, the mVC₈ reached 95.0%, earning the 1st place. Detailed results are presented in Tab. 6.



Category correction based on VLM		
		
User	Is the water in the image a river , lake or sea ? Please give me the only answer.	Is the water in the image a river , lake or sea ? Please give me the only answer.
GPT-4	The water in the image is a lake .	The water in the image is a sea .
LLAVA	The water in the image appears to be a river , as it is flowing and there is a visible waterfall, which is a common feature in rivers.	The water in the image appears to be a river , as indicated by the presence of a bridge in the background, which is a common feature along rivers in urban areas. The bridge’s design and the presence of buildings on the far bank also suggest that this is a river that runs through a city.

Table 5. **Ablation study of different VLM models.** We compare the examples and results of using different VLM models to correct challenging segmentation results. GPT-4 has higher recognition accuracy compared to LLAVA.

Team	mIoU	mVC ₈	mVC ₁₆
SiegeLion	67.8	<u>94.8</u>	92.9
Ours	<u>67.3</u>	95.0	<u>93.1</u>
kevin1234	63.9	<u>94.8</u>	93.3
bai_kai_shui	63.8	94.6	92.9
JMCarrot	63.4	94.6	92.9
ipadvideo	58.5	90.7	88.0

Table 6. **Comparisons with other teams on the final state.** The **first** and **second** highest scores are represented by bold font and underline respectively.

4. Conclusion

In this report, we present an innovative approach to enhance video segmentation performance. The Proposed training strategy Masked Video Consistency optimize the model’s utilization of temporal and spatial contextual cues in video segmentation tasks. By integrating Test-Time Augmentation (TTA) strategies, model aggregation and utilizing large multimodal models for post-processing, we enhance the robustness and accuracy of segmentation results, and explore the potential of other domain models in segmentation tasks. As a result, we obtain a significant improvements in both mIoU and video consistency metrics and achieve the 2nd place in the PVUW 2024 VSS track.

References

- Josh Achiam, Steven Adler, Sandhini Agarwal, Lama Ahmad, Ilge Akkaya, Florencia Leoni Aleman, Diogo Almeida, Janko Al-tenschmidt, Sam Altman, Shyamal Anadkat, et al. Gpt-4 technical report. *arXiv preprint arXiv:2303.08774*, 2023. 1, 3, 4
- Liang-Chieh Chen, Yukun Zhu, George Papandreou, Florian Schroff, and Hartwig Adam. Encoder-decoder with atrous separable convolution for semantic image segmentation. In *Proceedings of the European conference on computer vision (ECCV)*, pages 801–818, 2018. 4
- Bowen Cheng, Ishan Misra, Alexander G Schwing, Alexander Kirillov, and Rohit Girdhar. Masked-attention mask transformer for universal image segmentation. In *Proceedings of the IEEE/CVF conference on computer vision and pattern recognition*, pages 1290–1299, 2022. 3, 4
- Alexey Dosovitskiy, Lucas Beyer, Alexander Kolesnikov, Dirk Weissenborn, Xiaohua Zhai, Thomas Unterthiner, Mostafa Dehghani, Matthias Minderer, Georg Heigold, Sylvain Gelly, et al. An image is worth 16x16 words: Transformers for image recognition at scale. *arXiv preprint arXiv:2010.11929*, 2020. 2
- Gunnar Farneback. Two-frame motion estimation based on polynomial expansion. In *Image Analysis: 13th Scandinavian Conference, SCIA 2003 Halmstad, Sweden, June 29–July 2, 2003 Proceedings 13*, pages 363–370. Springer, 2003. 2
- Kaiming He, Xiangyu Zhang, Shaoqing Ren, and Jian Sun. Deep residual learning for image recognition. In *Proceedings of the*

- IEEE conference on computer vision and pattern recognition*, pages 770–778, 2016. 2
- Lukas Hoyer, Mauricio Munoz, Prateek Katiyar, Anna Khoreva, and Volker Fischer. Grid saliency for context explanations of semantic segmentation. *Advances in neural information processing systems*, 32, 2019. 2
- Dahun Kim, Jun Xie, Huiyu Wang, Siyuan Qiao, Qihang Yu, Hong-Seok Kim, Hartwig Adam, In So Kweon, and Liang-Chieh Chen. Tubeformer-deeplab: Video mask transformer. In *Proceedings of the IEEE/CVF conference on computer vision and pattern recognition*, pages 13914–13924, 2022. 4
- Xiangtai Li, Wenwei Zhang, Jiangmiao Pang, Kai Chen, Guangliang Cheng, Yunhai Tong, and Chen Change Loy. Video k-net: A simple, strong, and unified baseline for video segmentation. In *Proceedings of the IEEE/CVF Conference on Computer Vision and Pattern Recognition*, pages 18847–18857, 2022. 4
- Xiangtai Li, Haobo Yuan, Wenwei Zhang, Guangliang Cheng, Jiangmiao Pang, and Chen Change Loy. Tube-link: A flexible cross tube framework for universal video segmentation. In *Proceedings of the IEEE/CVF International Conference on Computer Vision*, pages 13923–13933, 2023. 4
- Haotian Liu, Chunyuan Li, Yuheng Li, and Yong Jae Lee. Improved baselines with visual instruction tuning. *arXiv preprint arXiv:2310.03744*, 2023. 1, 3
- Haotian Liu, Chunyuan Li, Qingyang Wu, and Yong Jae Lee. Visual instruction tuning. *Advances in neural information processing systems*, 36, 2024. 1, 3, 4
- Jiaxu Miao, Yunchao Wei, Yu Wu, Chen Liang, Guangrui Li, and Yi Yang. Vspw: A large-scale dataset for video scene parsing in the wild. In *Proceedings of the IEEE/CVF conference on computer vision and pattern recognition*, pages 4133–4143, 2021. 1, 3, 4
- Jiaxu Miao, Xiaohan Wang, Yu Wu, Wei Li, Xu Zhang, Yunchao Wei, and Yi Yang. Large-scale video panoptic segmentation in the wild: A benchmark. In *Proceedings of the IEEE/CVF Conference on Computer Vision and Pattern Recognition (CVPR)*, pages 21033–21043, 2022. 1
- Inkyu Shin, Dahun Kim, Qihang Yu, Jun Xie, Hong-Seok Kim, Bradley Green, In So Kweon, Kuk-Jin Yoon, and Liang-Chieh Chen. Video-kmax: A simple unified approach for online and near-online video panoptic segmentation. In *Proceedings of the IEEE/CVF Winter Conference on Applications of Computer Vision*, pages 229–239, 2024. 4
- Guolei Sun, Yun Liu, Henghui Ding, Thomas Probst, and Luc Van Gool. Coarse-to-fine feature mining for video semantic segmentation. In *proceedings of the IEEE/CVF conference on computer vision and pattern recognition*, pages 3126–3137, 2022a. 4
- Guolei Sun, Yun Liu, Hao Tang, Ajad Chhatkuli, Le Zhang, and Luc Van Gool. Mining relations among cross-frame affinities for video semantic segmentation. In *European Conference on Computer Vision*, pages 522–539. Springer, 2022b. 4
- Yuetian Weng, Mingfei Han, Haoyu He, Mingjie Li, Lina Yao, Xiaojun Chang, and Bohan Zhuang. Mask propagation for efficient video semantic segmentation. *Advances in Neural Information Processing Systems*, 36, 2024. 4
- Tao Zhang, Xingye Tian, Yu Wu, Shunping Ji, Xuebo Wang, Yuan Zhang, and Pengfei Wan. Dvis: Decoupled video instance segmentation framework. In *Proceedings of the IEEE/CVF International Conference on Computer Vision*, pages 1282–1291, 2023a. 1, 4
- Tao Zhang, Xingye Tian, Yikang Zhou, Shunping Ji, Xuebo Wang, Xin Tao, Yuan Zhang, Pengfei Wan, Zhongyuan Wang, and Yu Wu. Dvis++: Improved decoupled framework for universal video segmentation. *arXiv preprint arXiv:2312.13305*, 2023b. 1, 2, 3, 4